

QUANTUM COMPUTING AND QUANTUM INFORMATION- QUANTUM INFORMATION PROCESSING WITH PHOTONIC QUBITS: EXPLORING THE USE OF PHOTONIC QUBITS FOR QUANTUM INFORMATION PROCESSING

Mohd. Shakil Qureshi^{1*}, P. Hari Krishna², Bhavana Kshirsagar³, Saket Jain⁴, Medhavi Bhargava⁵

¹Department of Physics, Medicaps University, Indore, Madhya Pradesh, India, shakil@medicaps.ac.in

²Department of Physics, Medicaps University, Indore, Madhya Pradesh, India, phari.krishna@medicaps.ac.in

³Department of Physics, Medicaps University, Indore, Madhya Pradesh, India, bhawna.kshirsagar@medicaps.ac.in

⁴Department of Computer Science & Engineering, Lakshmi Narain College of Technology Excellence, Bhopal, Madhya Pradesh, India, saketjains130579@gmail.com

⁵School of Engineering and Technology, Sanjeev Agrawal Global Educational (SAGE) University, Bhopal, Madhya Pradesh, India, medhavibh14@gmail.com

Corresponding Author: Mohd. Shakil Qureshi (Email: shakil@medicaps.ac.in)

Abstract: Compared with other physical platforms for Quantum Information Processing (QIP), photons have the unique advantages of travelling over free-space links or optical fiber with relatively low decoherence and of propagating with minimal coupling to the environment, while also being easily coupled to existing telecommunications technology. The R&D of various single photon and entangled photon generation technologies and the linear-optical implementations of quantum computation and communication are now surveyed and analyzed in a structured manner. We discuss photonic qubit degrees of freedom (polarization, time-bin, path, frequency and Orbital angular momentum), determine sources such as deterministic quantum-dot based sources and probabilistic sources based on spontaneous parametric down conversion (SPDC), and review architectures for Linear Optical Quantum Computation (LOQC), such as the Knill–Laflamme–Milburn (KLM) protocol and measurement-based quantum computation. Building on the density-matrix treatment of biexciton–exciton coherent dynamics in semiconductor quantum dots, we recapitulate the development of two-pulse coherent control schemes for generation and readout of photonic qubits in these systems and how they have been stretched towards optical control of logic gates. A comparative performance framework is established along the lines of source brightness, entanglement fidelity, photon indistinguishability, channel loss and scalability, which is illustrated by simulated performance plots and tabulated against literature numbers. Remaining hurdles in the field regarding issues of photon loss, scalable multiplexing, deterministic two-qubit interaction, and its integration with a quantum memory are highlighted and a perspective is provided on hybrid photonic–matter architectures for fault-tolerant quantum networks...

Keywords: Photonic qubits, Quantum Information Processing, Linear Optical Quantum Computing, Quantum Dots, Entangled Photon Sources, Quantum Key Distribution, Density Matrix, Biexciton, Hong–Ou–Mandel Interference



1. INTRODUCTION

The aim of Quantum Information Processing (QIP) is to use superposition, entanglement and interference to do what can not be done efficiently or securely classically. Many different physical systems (such as superconducting circuits, trapped ions, neutral atoms, semiconductor spin qubits) have been showing fast improvements in gate fidelity, but the only material to date capable of operating at such distances as to carry quantum information is photons and they are still key to any future quantum internet.

For QIP there are a number of attractive properties of photons. These remain almost unaffected at room-temperature thermal environment and can propagate with the light speed, build-up low intrinsic dephasing and can be encoded simultaneously in several independent degrees of freedoms such as polarization, temporal (time-bin), spatial (path), frequency, and Orbital Angular Momentum (OAM) modes [1] [2]. Such properties make photons natural candidates for Quantum Key Distribution (QKD), quantum teleportation, distributed quantum computing, and allow for operation at room temperature which is hard to achieve for matter based qubits [11] [12].

Yet, because of the same weak photon–photon interaction responsible for the stability of the photonic qubits, deterministic gates between pairs of qubits are challenging to achieve directly with single photons, particularly given the extremely weak nature of optical nonlinearities at the singlephoton level [2]. The first breakthrough, proposed by Knill, Laflamme and Milburn (KLM), proved that nonlinear two-qubit gates could be simulated with only linear optical components, such as beam splitters and phase shifters, plus photon counting and post-selection, which ushered in the era of linear optical quantum computing (LOQC) [3] [2] [13] [14]. One such insight was that instead of "engineering strong photon nonlinearities," the central engineering issue of photonic QIP becomes "efficient detectors, low-loss linear optical networks, and high quality single photon sources.

The second key photonic QIP idea is the generation of a single and entangled photon. There are two main methods: probabilistic generation from Spontaneous Parametric Down-Conversion (SPDC) in a nonlinear crystal and deterministic generation from solid-state devices, e.g., Semiconductor Quantum Dots (QDs). Coherent control of exciton and biexciton states can be used to obtain controlled, on-demand emission of single photons and of entangled pairs of photons, and the development, both theoretical and experimental, of quantum-dot sources of such photons and pairs has received significant attention in the past few years.

The development of heralding and multiplexing electronics, as well as high efficiency superconducting nanowire single photon detectors and low-loss integrated photonic waveguide platforms have also advanced in parallel and contributed to the growing interest in photonic QIP. These developments have made photonic QIP move away from the proof-of-principle, bulk-optics approach to chip-scale and field deployable systems, enough to warrant the systematic comparison sought in the present paper. Specifically, it is important to have a way to relate the predictions of the physico-mathematical models of the solid state to more concrete measurement parameters for sources and gates such as its peak output and the time it takes to respond to an external control parameter.

A simple density matrix model of a single semiconductor quantum dot was theoretically investigated by Sen, Qureshi, and Sen to describe a two-pulse excitation sequence that can populate a biexciton state through two photon absorption and then transfer to the exciton state through stimulated emission [4]. In follow-up work, Qureshi et al. extended this density-matrix scenario to investigate the implementation of all-optical quantum controlled-NOT (CNOT) gate in a single quantum dot for the ground, exciton, and biexciton states as the pseudo-logical bits for the control and target pulses [5]. These two works present a concrete physical realization of how the generation of photonic-qubits (by the biexciton cascade) and the photonic/excitonic logic (also by stimulated emission and pulse-area control) can be combined in a single solid-state platform and thus serves as an important reference for the more general comparison presented in this paper.

The rest of this paper is structured as follows. The review of the physical realisations of the various photonic qubit encodings is presented within Section II. In Section III, techniques for generating single photons and entangled photons are discussed, focusing on the quantum-dot biexciton cascade and SPDC. Section IV gives a survey of the linear optical quantum computing architectures and the linear optical gate constructions, including the use of the coherent control schemes discussed in [4] and [5]. The research methodology used in this work is presented in section V. A comparative performance analysis with tables and illustrative graphs is presented in Section VI. Section VII presents some future directions, Section VIII discusses and analyzes the results and Section IX presents some concluding remarks.

Notation and Symbols

Symbols used in Sections III and V and representative of the quantities shown later in this paper are listed in Table 0 below for the benefit of the reader wishing to follow the actual physical origin of the figures involved in the simulation of the illustrative cases.

Symbol	Meaning
$\rho_{bb}(t)$	Biexciton state population density at time t
$\rho_{ee}(t)$	Exciton state population density at time t
T_2	Dephasing (coherence) time of the quantum-dot states
α, β	Rabi frequencies associated with the first and second excitation pulses
τ_c	Coarse time delay between the first (control) and second (target) pulses
Ω_1	Generalized Rabi frequency, $\Omega_1^2 = \alpha^2 + \beta^2 + \Delta^2 + T_2^{-2}$
Δ, Δ'	Detuning parameters for the first and second pulse transitions
x, y	Decay-rate parameters governing the oscillatory terms in $\rho_{bb}(t)$ and $\rho_{ee}(t)$

2. PHOTONIC QUBIT ENCODINGS

A photonic qubit is the two-dimensional (or effectively two dimensional) Hilbert space, which is encoded in some degree of freedom of a single photon, or photon mode. The robustness to certain noise channels, like fibre birefringence or timing jitter, and what optical elements are possible for the encoding, manipulation and measurement of the state in this way is determined by the chosen encoding.

A. Polarization Encoding

the logical state $|0\rangle$ is related to the photon being horizontally (H) polarized and $|1\rangle$ is related to the photon being vertically (V) polarized. Wave plates are used to perform arbitrary single-qubit rotations and polarizing beam splitters combined with single-photon detectors are used for the measurement. Polarization encoding is the most common scheme in free space and short distance fiber experiments because of the simple optical elements involved, but effects such as polarization mode dispersion and polarization birefringence drift are present in standard telecom fiber for a long distance, and if not actively corrected for, could be problematic.

B. Time-Bin Encoding

The qubit is encoded in the arrival time of a photon in either of 2 (or more) temporal slots created by an unbalanced interferometer. As the photon in both time bins resides in the same spatial and polarization mode, the time bin qubits are a very promising choice for fiber-based QKD and quantum networking requiring propagation over long distances, where polarization-mode dispersion in the optical fiber may become relevant.

C. Path (Dual-Rail) Encoding

In path encoding, the logical state is encoded in the presence or absence of the photon in one of two spatial modes (fibre paths or waveguides). All the discussions of the KLM protocol implicitly assume a dual-rail encoding, which is the natural representation in an integrated photonic circuit, where phase shifters and beam splitters have a direct effect on spatial mode amplitudes.

D. Frequency-Bin Encoding

Methods such as frequency encoding can be used to encode a photon with different logical states via different spectral modes, which are controlled using the electro-optic modulators and pulse shapers. Frequency-bin (or frequency-encoded) photonic qubits can also, in principle, enable parallel multi-qubit gate operations within a single spatial channel – a feature dubbed as spectral linear optical quantum computation – and can be transmitted over wavelength-division-multiplexed fiber systems.

E. Orbital Angular Momentum (OAM) Encoding

The OAM encoding takes advantage of the helical phase structure of Laguerre–Gaussian photon modes, which in principle can be put on a high dimensional (qudit) Hilbert space, as opposed to a fixed 2-level qubit [21]. OAM encoding and its potential applications in high-dimensional QKD and in augmenting channel capacity per photon are appealing [22] [23], but OAM propagation is more sensitive to the atmosphere turbulence in free space and modal cross-talk in standard fiber.

Summary Comparison of Encodings

Table I : Summarizes the Principal Trade-Offs among the Five Encodings Discussed above

Encoding	Typical Manipulation Optics	Key Advantage	Key Limitation
Polarization	Wave plates, PBS	Simple state preparation/readout	Fiber birefringence drift
Time-bin	Unbalanced interferometer	Robust to polarization dispersion	Requires stable interferometric phase
Path (dual-rail)	Beam splitters, phase shifters	Natural for integrated photonics	Mode-matching loss in chip coupling
Frequency-bin	EOM, pulse shaper	WDM-compatible, parallel gates	Requires precise spectral control
OAM	Spatial light modulators, q-plates	High-dimensional encoding (qudits)	Turbulence and modal cross-talk

3. SINGLE-PHOTON AND ENTANGLED-PHOTON SOURCES

The controllable creation of single photons and entangled photon pairs is essential to almost all QIP protocols via photons. A current trend in research involves making two kinds of source: (1) probabilistic nonlinear-optical sources, which rely on the process of spontaneous parametric down-conversion, or (2) deterministic solid-state emitters, which are realized from semiconductor quantum dots.

A. Spontaneous Parametric Down-Conversion (SPDC)

SPDC is a process that uses a second order nonlinear crystal, which is illuminated by a strong laser pulse, to probabilistically produce “superradiant pairs” of photons entangled in certain degrees of freedom (e.g. polarization) [6] [7]. The created signal can be well modeled by an random sequence of photon pairs, with inevitably high probability of having more than one pair within a single detection window [6]. The compromise between the number of generated photons (brightness) and the number of photons per mode (photon-number purity) naturally restricts SPDC sources for mid- to long-range quantum networking [7].

B. Quantum-Dot-Based Sources and the Biexciton Cascade

Through the radiative decay of a biexciton state, to an exciton state and then finally to the ground state, semiconductor quantum dots can deterministically generate single photons or entangled photon pairs [7] [8] [15]. The “on demand” emission of photons from the biexciton cascade after a single excitation pulse avoids the multi-pair

emission issue of SPDC, and can in principle be close to unity provided additional photonic antenna or cavity structures are used in conjunction with these sources.

Sen, Qureshi and Sen came up with a simplified 6×6 density-matrix model (compared to the conventional 9×9 model) of the population transfer from the continuum to the biexciton ($2 \rightarrow 0$) and subsequently to the exciton ($1 \rightarrow 0$) state of the $\text{In}_{0.5}\text{Ga}_{0.5}\text{As}/\text{GaAs}$ Quantum Dot (QD) through the process of two photon absorption (TPA) by a first pulse followed by the process of stimulated emission by a second pulse with a delay time between them [4]. They find from their analysis that the population of biexcitons displays Rabi-type oscillations with a decay rate that timescale T_2 of dephasing, and that the population of the exciton state is a modulated wave whose envelope frequency is determined by the frequency of the weak pulse (the target) while the frequency of the faster carrier oscillation is determined by the frequency of the strong pulse (the control). These results are consistent with the experiment results of Rabi oscillations and quantum interference found for $\text{InGaAs}/\text{GaAs}$ and CdSe/ZnSe quantum dots.

This density-matrix model qualitatively can reproduce the population dynamics of the biexciton system shown in Figure 1 below: an initial Rabi-like oscillation which decays to a steady biexciton population for increasing pulse delays beyond the dephasing time.

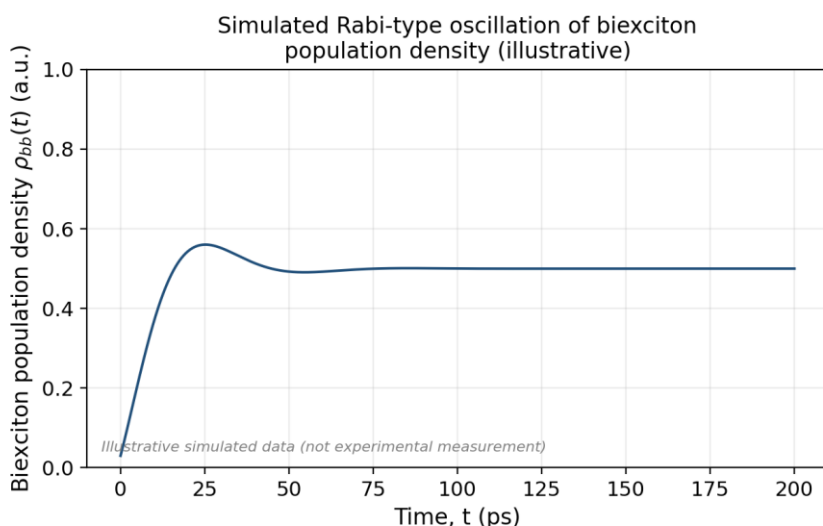


Fig. 1. Simulated biexciton population density vs. time, illustrating the Rabi-type oscillatory decay qualitatively consistent with the two-pulse coherent-control model of [4]. Curve is simulated for illustration and is not raw experimental data

Based on the same coherent-control framework, Qureshi et al. (Sen, G. Jarra, et al.) proposed and analyzed a single-SEMQRD implementation of the two-bit logical operation (or CNOT gate) using the first (control) pulse and the second (target) pulse on the basis states $|00\rangle$, $|01\rangle$, $|10\rangle$, and $|11\rangle$ where absence/presence of each pulse corresponds to the basis state [5]. The density-matrix solution of their model reveals that the biexciton population oscillates as a superposition of two frequency components, labeled a and b, respectively, where the effective Rabi frequency is no longer a well-defined frequency corresponding to population inversion that can in principle be reached. Even within this thresholded population criterion under which the above-mentioned input-output truth table was shown, the device can be considered to approximate the action of the CNOT gate on photonic/excitonic logical states: The $|10\rangle$ input state results in population of the biexciton state through the process of two-photon absorption, while the $|11\rangle$ input state produces stimulated emission to the exciton state.

C. Comparative Source Performance

Recently, quantum-dot sources have been demonstrated with coincidence levels reaching the megapair per second regime and post-selected entanglement fidelities of more than 98% [8] [16] [17] [19] [20] closing the gap between photon rates historically achieved with SPDC sources and the brightness of quantum-dot sources, while maintaining their low multi-photon emission probability. Telecom-band sources of such QTs with collection efficiencies better than $\sim 30\%$ were estimated to out-perform classic QKD based on an SPDC source over the same channel [9].

Representative ranges for the two source paradigms, informed by literature are given in comparison for various performance measures relevant for QIP applications in Table II.

Metric	SPDC Sources	Quantum-Dot Sources
Generation statistics	Probabilistic (Poissonian pairs)	Deterministic (on-demand, per pulse)
Multi-photon emission risk	Present at higher pump power	Intrinsically suppressed
Typical pair/photon rate	Low per-pulse probability, scalable pump power	High per-pulse probability, fixed by emitter dynamics
Reported entanglement fidelity	Up to ~98% in optimized setups	Up to ~98% in optimized post-selected setups
Operating temperature	Room temperature	Cryogenic (typically <10 K)
Spectral tunability	High (crystal/phase-matching dependent)	Limited by emitter growth and Stark tuning
Photon indistinguishability control	High, via filtering	High, with resonant excitation and Purcell enhancement

4. LINEAR OPTICAL QUANTUM COMPUTING AND PHOTONIC LOGIC GATES

A. The KLM Protocol and Measurement-Induced Nonlinearity

At the single photon level, direct photon–photon interaction in the presence of the weak nonlinearities is impractical using current materials [2]. In the KLM protocol, this is achieved without any nonlinear optics by only employing linear optical elements (beam splitters and phase shifters), auxiliary (ancilla) photons, and photon-number-resolving detection along with post-selection and heralding to realize an effective nonlinear optical phase gate [3] [2] [11]. Although the resulting two-qubit operations are probabilistic, they are only successful upon certain and sufficient detection outcomes, the protocol was demonstrated to be scalable to universal quantum computation with the aid of plenty of ancillas and feed-forward control mixing [14].

B. Measurement-Based Quantum Computation with Photonic Graph States

The other architecture is called "Measurement-based Quantum computation" or MBQC, in which an entangled multi-photon cluster or graph state is prepared first and computation is done just with adaptive single qubit measurements [1] [13]. Photonic graph states are regarded as essential resources for error corrected fully photonic quantum computation, in which time consuming entangling operations are performed before the computation and not "on-demand" during it.

C. Coherent-Control-Based Logic in Quantum Dots

One potential path towards the "photon-passive" logic is to use coherent control of matter qubits (excitons/biexcitons), which then emit/absorb photons in a controlled manner. The proposal of the quantum-dot CNOT gate in [5] exploited the ground–exciton–biexciton manifold of only one QD, where the absence/presence of two successive optical pulses are considered as input control and target bits, respectively. The latter approach is fundamentally different from KLM-type LOQC, in that, instead of passively using linear optics to manipulate already flying photonic qubits, the quantum dot's internal state is manipulated directly, with the output cascade photon serving as the signal that reports the logical outcome, the pulse area, detuning, and pulse delay operating as control parameters.

This difference is illustrated in Table III, where pure LOQC-type photonic logic gates are compared to coherent-control based logic with a quantum dot mediator as studied in [4] and [5].

Property	LOQC / KLM-type Gates	QD Coherent-Control Gates [4],[5]
Information carrier during gate operation	Flying photons in linear optical network	Bound exciton/biexciton states in solid-state emitter
Nonlinearity source	Measurement-induced (photon counting + post-selection)	Intrinsic optical nonlinearity of two-photon absorption
Control parameters	Beam-splitter reflectivity, phase shifts	Pulse area, detuning, pulse delay (τ_c)
Determinism	Probabilistic (success conditioned on detection)	Deterministic in principle, limited by dephasing T2
Readout	Direct photon detection	Photoluminescence from biexciton/exciton decay

D. Photon Indistinguishability and Two-Photon Interference

The near-perfect indistinguishability of independently generated photons is an important feature of many LOQC gates, and for all entangled-photon generation schemes based on interference. Usually, this is accomplished by Hong Ou Mandel (HOM) interference--when two photons arrive at the beam splitter from different arms, one bunch together into the same output beam splitter, which is simply a dip in the coincidence count as a function of the relative arrival time [18]. The qualitative shape of such a HOM interference dip is shown in figure 2.

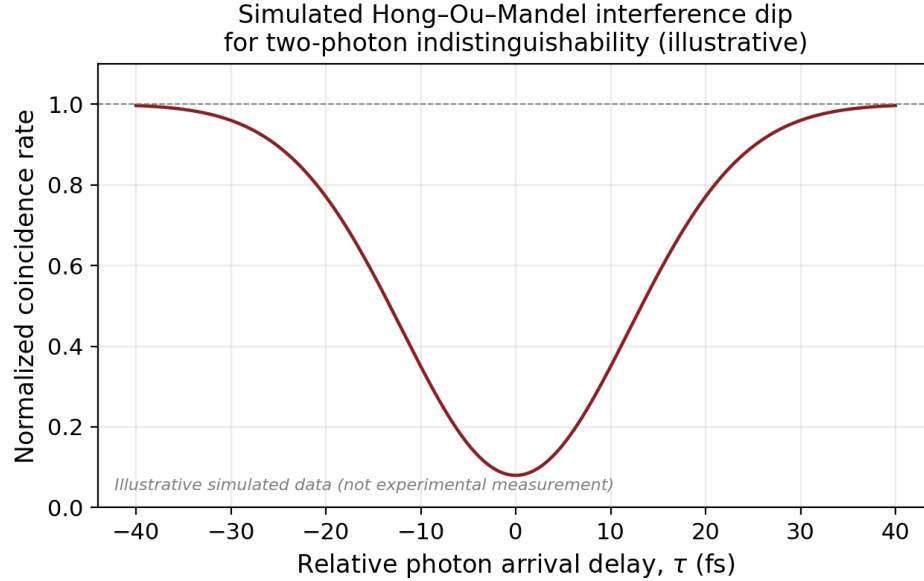


Fig. 2. Simulated Hong–Ou–Mandel coincidence dip illustrating two-photon interference visibility used to certify photon indistinguishability. Curve is simulated for illustration and is not raw experimental data.

5. RESEARCH METHODOLOGY

The work is of the literature survey and comparative study nature, typical for a subject which is spread across a theoretical density-matrix description of sources, experimental source characterizations, and architectural comparisons of different quantum-computing schemes. The steps in the methodology can be executed in 9 steps, shown in the flowchart of Figure 3.

Stage 1 serves as a research scope — the main photonic qubit encodings are outlined and the QIP tasks of interest are identified: computation, communication and key distribution. In stage 2, the literature is surveyed in IEEE Xplore, arXiv, APS journals, Nature Publishing Group journals and AIP Publishing journals; in particular the focus is on theoretical and experimental work on quantum dots, SPDC sources and linear optical architectures that has been peer-reviewed. Stage 3 categorizes the investigated photonic encoding of qubits based on the degree of freedom. Stage 4 compares deterministic quantum-dot emission with probabilistic SPDC, with maps of the light-single photon and entangled-photon sources. Stage 5 lists those quantum gate and logical processing schemes that are suitable: KLM-type LOQC, measurement-based quantum computation, and coherent-control-based quantum-dot logic gates that were reported in [4] and [5].

In stage 6 a comparison structure is built up ranging from fidelity, steady state generation of photons, channel loss, scalability and decoherence behaviour and dephasing behaviour. In stage 7, illustrative simulation models are constructed based on the governing physical equations, namely, a density-matrix model for Rabi-oscillation in the population dynamics of biexcitons as described in Ref. [4], a classical Hong-Ou-Mandel interference model for photon indistinguishability, and the standard exponential attenuation model for fiber-optic channel loss. These were simulated curves, which are explicitly illustrative only, and are not copies of any specific experimental finding; the fact that they are simulated, and not reproductions of any actual experimental finding is indicated in each figure. Stage 8 is a tabulation of performance ranges reported in the literature and allows to make comparative plots. Finally, at stage 9, the results are summarized and discussed in sections VII-IX as regards the open challenges and future directions.

A. Governing Relations Used for Illustrative Modeling

The biexciton-population curve of Figure 1 is modelled qualitatively after the analytical solution of the reduced 6×6 density-matrix equation of motion reported in [4] in which the density $p_{bb}(t)$ evolves as a sum of a steady state term and a decaying oscillatory term with frequency $\sqrt{3}x$ and decay rate x , and additional exponential decaying terms with decay rate $2/T_2$, where x itself is proportional to the cube root of the ratio $(\alpha^2/\Omega_1^2, \beta^2/\Omega_1^2)$ of the squared Rabi frequencies to the squared generalized Rabi frequency, and the dephasing time T_2 . The parameter values used in

Figure 1 were chosen for illustrative purposes, with overall trends in the decay envelope and in the oscillation period mimicked qualitatively those reported for InGaAs/GaAs quantum dots in [4] without trying to reproduce the specific numerical curve from any one of the figures in the source paper.

The Hong–Ou–Mandel dip of Fig. 2 is described by the normalization of the standard Gaussian-overlap approximation for the normalized coincidence rate as function of the relative delay of the photons, τ , described by the parameter of visibility V and the coherent time that corresponds to the bandwidth of the photons. The fiber-loss curve in Fig. 5 is as per the following exponential attenuations law $T(L) = 10^{-(\alpha L/10)}$ where α is 0.2dB/km which represents the standard single-mode telecom fiber at 1550nm. The behaviour of this exciton-population curve in Figure 6 qualitatively agrees with that given previously for $\rho_{ee}(t)$ in [4] in which a slower envelope function – controlled by the weaker second pulse – is multiplied by a faster carrier oscillation – controlled by the stronger first pulse.

B. Parameter Sensitivity Considerations

The qualitative feature of the simulated curves shown in Section VI (the shape of the curves) depends strongly on the dephasing time T_2 , as well as on the Rabi frequencies α and β (proportional to the pulse amplitude), so that in a real device it will vary with the sample temperature and with the excitation intensity. In particular, the higher the Rabi frequencies compared to the dephasing rate T_2^{-1} the more pronounced the oscillations before decay, revealing that the condition given for the observable Rabi oscillations in the quantum-dot CNOT-gate analysis, [5] $\sqrt{8T_2\alpha} \geq 1$, is fulfilled. This sensitivity is not a problem that is unique to this paper, but only part and parcel of any reduced order analytical model of this kind: any such model holds valid only in the same high field, near resonant excitation regime as the original derivations.

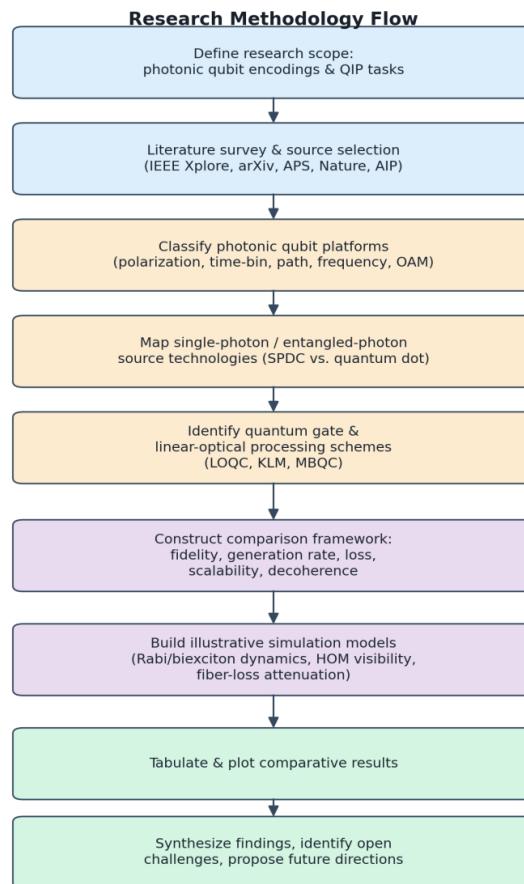


Fig. 3. Research Methodology Flow Diagram Followed in this Study

6. COMPARATIVE PERFORMANCE ANALYSIS

A. Source Brightness vs. Entanglement Fidelity

One of the main issues in the design of photonic QIP is the possible trade-off between the extraction efficiency (brightness of the source), typically defined as the probability of producing a useful pair of photons per pump pulse, and the fidelity of the entanglement. Comparisons in the literature plot these two against one another for sources of SPDC and from quantum dots: In general, the sources of SPDC tend to bunch together at low brightness with high achievable fidelity, while the sources using quantum dots show a wider brightness range due to the continuous strategies for increasing the efficiency of optical antenna and cavity extraction. The qualitative trend shown here is illustrated by an illustrative scatter plot in which the value of the specific data points are simulated for illustrative purposes only, and should not be construed as representative of any particular publication's measured values as shown in the figure.

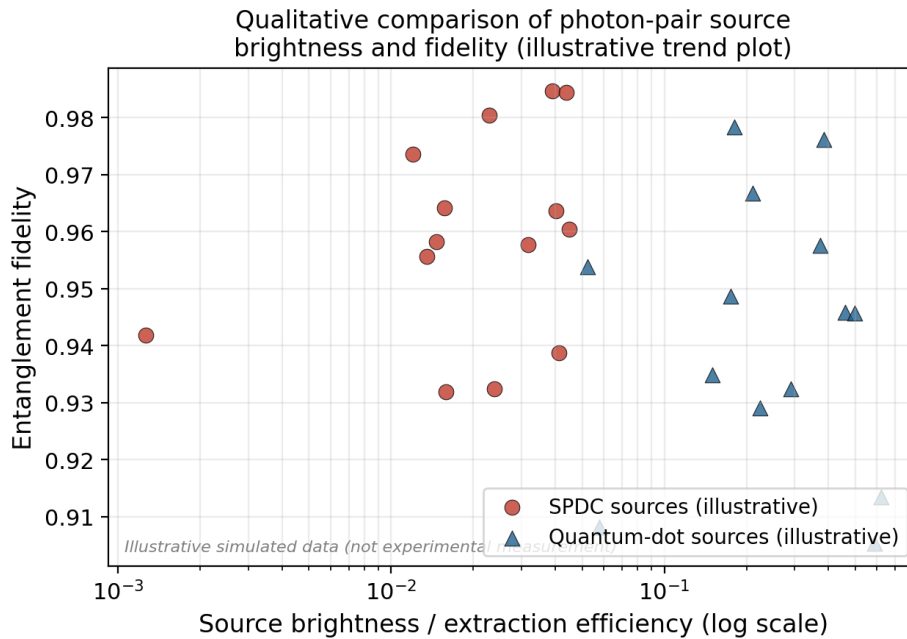


Fig. 4. Illustrative comparison of source brightness/extraction efficiency vs. entanglement fidelity for SPDC and quantum-dot sources. Data points are simulated to reflect qualitative literature trends and do not represent specific measured values.

B. Channel Loss and Distance Scaling

The primary resource cost is the loss of photons, for any photonic QIP protocol operating in fiber the losses grow exponentially with distance (because fiber ex always attenuates photons; at the telecom wavelength of 1550 nm the current standard telecom fiber parameter is ~ 0.2 dB/km). That's this standard attenuation model shown in Figure 5, indicating the importance of quantum repeaters and quantum memories for fibre-based quantum networks in total distances longer than a few tens of kilometres.

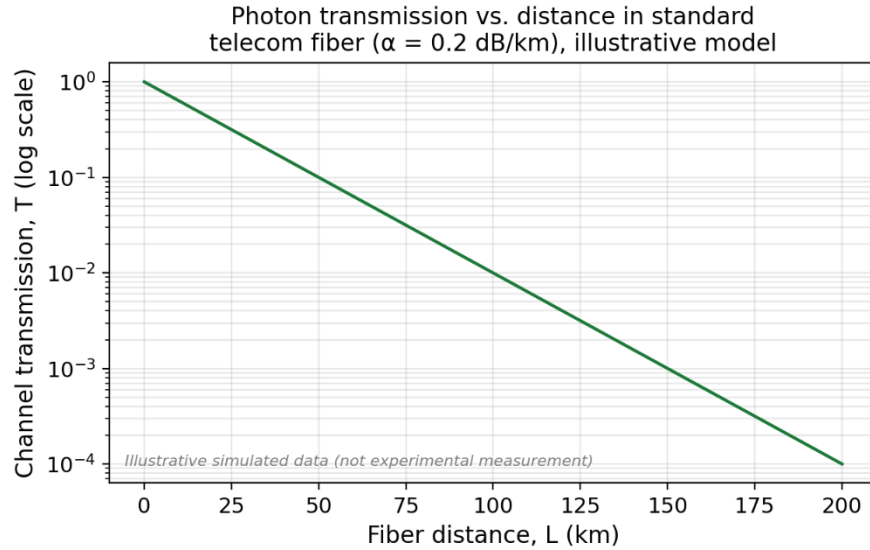


Fig. 5. Photon transmission probability vs. fiber distance under the standard telecom attenuation model ($\alpha = 0.2$ dB/km). This is a standard physical model, not an experimental measurement.

C. Exciton State Population Dynamics Under Two-Pulse Excitation

Within the coherent-control quantum-dot framework of Section III-B, the exciton-state population reported in [4] has a form of modulated wave with a slow amplitude envelope determined by the (weak) second pulse and a fast oscillatory envelope determined by the (strong) first pulse and describes the superposition of the biexciton and exciton Rabi dynamics. This modulation of the wave in a qualitative manner is displayed in Figure 6.

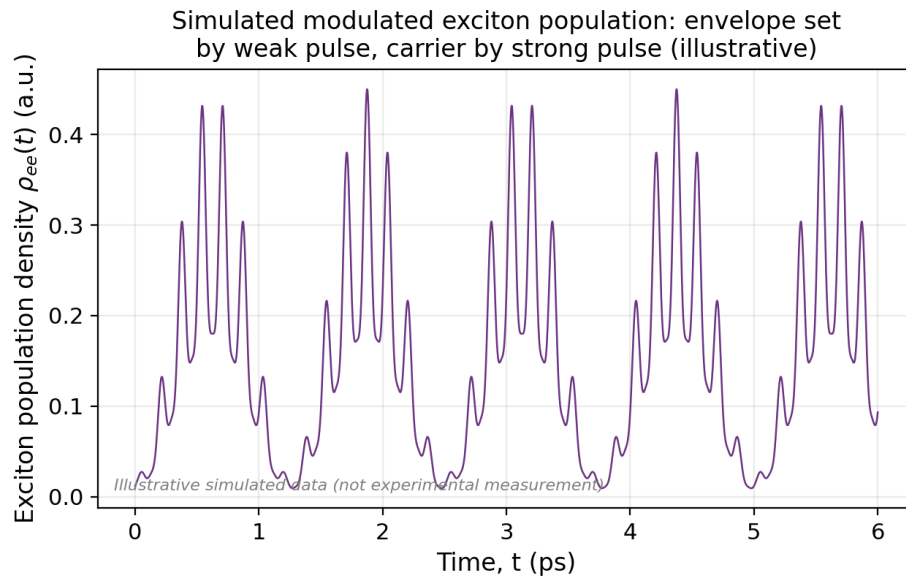


Fig. 6. Simulated exciton-state population showing a modulated-wave envelope/carrier structure, qualitatively consistent with the two-pulse excitation model of [4]. Curve is simulated for illustration.

D. Consolidated Comparison Table

Table IV provides a comparative metrics reference table throughout source technologies and processing architectures to summarize the metrics relative to each section of the paper (Sections III, IV, and VI).

Approach	Determinism	Typical Fidelity Range	Primary Loss Mechanism	Scalability Outlook
SPDC entangled-photon source	Probabilistic	~93%–98%	Low extraction at high purity	Limited by multi-pair emission at scale
Quantum-dot biexciton cascade [4],[5]	Deterministic (per pulse)	~90%–98%	Cavity/antenna extraction efficiency	Improving with photonic engineering
KLM/LOQC two-qubit gate	Probabilistic (post-selected)	Architecture-dependent	Ancilla overhead, photon loss	Resource-intensive but theoretically universal
MBQC with photonic graph states	Deterministic computation, probabilistic state prep	Architecture-dependent	Cluster-state generation loss	Promising for fault tolerance
QD coherent-control logic [5]	Deterministic in principle	Bounded by dual-frequency Rabi dynamics	Dephasing time T_2	Single-emitter scaling remains open

E. Applications: QKD, Teleportation, and Distributed Computing

Any approach that relies on data integrity across transactions will experience some amount of degradation in fidelity, which will also depend on how the data is accessed.

1) Quantum Key Distribution

Entanglement-based QKD protocols, for example BBM92, involve two parties using entangled pairs of photons to generate a secret key, but it is not the source assumption that is used to guarantee the security, but rather the violation of the Bell-type inequality [6] [23]. Thus the achievable secure key rate depends on the pair generation rate, on the channel transmission (Fig. 5), on the detector efficiency, and also on the probability for emission of multiple pairs by the source, and this fact means the SPDC-vs-quantum-dot brightness/fidelity trade-off discussed in Section VI-A directly translates into the actual QKD performance at a given distance.

2) Quantum Teleportation and Entanglement Swapping

The former, called quantum teleportation, is a process that allows the transfer of an unknown qubit state between distant parties based on a shared entangled pair of qubits and classical communication, and the latter, or entanglement swapping, is a way of building up entanglements between several pairs of intermediate nodes (e.g., photons) without transferring the photons over the entire distance. Both protocols require high indistinguishability at the Bell-state measurement stage: imperfect indistinguishability directly close to the Bell-state measurement stage directly affects the fidelity of the swapped or teleported state, and the indistinguishability properties of the sources have recently been benchmarked with reference to entanglement-swapping applications.

3) Distributed and Networked Quantum Computing

When coupled with photonic interconnects, this enables multiple, small-scale quantum processors to be connected, enabling computational resources to be distributed among processors where the physical qubit modality

does not need to be the same in each. In such architectures, the "photon" is used merely as a matter and communication medium entangling two nodes for a processing event, which means that the brightness, fidelity, and loss of the photons in Sections VI-A through VI-C are directly related to the entangling-gate rate that can be achieved between nodes for the distributed computation.

For convenience, the dominant application-level requirement that is limiting for each class of applications is summarized in Table V, which is a useful cross-reference between the architectural comparison of Table III/IV and the application-level requirements described within this sub-section.

Application	Dominant Limiting Metric	Most Relevant Source Property
Entanglement-based QKD	Secure key rate vs. distance	Multi-pair emission probability, channel loss
Quantum teleportation	Teleportation fidelity	Photon indistinguishability (HOM visibility)
Entanglement swapping / repeater nodes	Swapped-state fidelity, swap rate	Source brightness and spectral matching
Distributed quantum computing	Inter-node entangling-gate rate	Combined brightness, loss, and detector efficiency

F. Integrated Photonic Circuit Platforms

A parallel and growing important trend in the study of photonic QIP is the efforts to translate bulk-optics demonstrations onto integrated photonic chips that are manufactured in silicon, silicon nitride, silicon photonics on insulator, and lithium niobate. The very same issues brought up in Section VII (scalability, free space and fiber-coupled bulk components, beam splitter, phase shifters and waveplates, and wafer-scale compatibility) can be answered by integration.

1) Waveguide-Based Linear Optical Networks

Reconfigurable waveguide meshes with arbitrary unitary transformations on arbitrarily encoded photonic qubits have been demonstrated by integrated thermo-optics or electro-optics phase shifters in addition to integrated directional-couple beam splitters. This type of circuit directly encodes all the passive linear-optical layer necessary for the KLM-type of LOQC-like architectures described in Section IV-A, and has been applied to small scale quantum gates, Boson-sampling experiments and reconfigurable quantum walks on the single-chip level.

2) On-Chip Single-Photon Sources and Detectors

On-chip photon-pair sources like spontaneous four-wave mixing (FWM) in silicon nitride micro-ring resonators, or directly integrating quantum-dot emitters in photonic-shaped structures, are starting to be integrated into integrated photonic platforms. The direct coupling of superconducting nanowire single photon detectors (SNSPDs) to waveguides also removes losses associated with the hybrid bulk-to-fiber-to-chip architectures, directly tackling the problem of (channel) loss that otherwise dominates in such hybrid architectures as illustrated in figure 5.

3) Heterogeneous Integration of Quantum-Dot Emitters

Studies addressing the transfer of coherent-control schemes, as in [4] and [5] to an integrated waveguide geometry, where the excitation pulses and the emitted single photon are guided in an integrated fiber or free space, are of special interest because of the excellent single-atom isolation in the reflective cavity geometry that was employed in the experiments of these citations. Given the excellent single-atom isolation provided by the reflective cavity geometry used in the experiments of these citations, an important open engineering question is whether logic involving coherent control by two pulses can be transferred into an integrated waveguide geometry in which the excitation pulses and the emitted single photon are guided on-chip rather than by free space. While the high-field, near-resonant excitation conditions required by the density-matrix description adopted in [4] and [5] is a challenging and ongoing geometry engineering effort for achieving full integration, the effort to deterministically arrange quantum dots in the photonic crystal cavity and waveguides is progressing well.

A summary of the four major classes of the architecture that are surveyed in this paper in terms of footprint, phase stability, and their current state of maturity are provided in Table VI.

Architecture	Footprint	Phase Stability	Maturity Level
Bulk-optics LOQC	Large (optical table scale)	Sensitive to vibration/thermal drift	Mature for small-scale demonstrations
Integrated waveguide circuits	Chip scale (mm–cm)	Inherently stable, lithographically fixed	Rapidly maturing; growing qubit counts
Quantum-dot coherent-control logic [4],[5]	Single-emitter, cryostat-scale	High coherence within T2 window	Demonstrated theoretically; single-emitter scaling open
SPDC entanglement distribution	Crystal + filtering optics	Moderate, filtering-dependent	Mature, widely deployed in QKD testbeds

7. OPEN CHALLENGES

Nevertheless, there are a lot of problems to be overcome to make the scalability of photonic QIP feasible.

A. Photon Loss and Channel Capacity

The multiplications of fiber attenuation and component insertion loss directly lead to a decrease of the success probability of probabilistic gates and the secure key rate in the QKD links across long optical networks and large-scale linear-optical circuits.

B. Deterministic Photon-Photon Interaction

The difficulty of photonic two-qubit gates [2] is the absence of robust and low-loss optical nonlinearities at the single-photon level. One way ahead is to use hybrid schemes in which photons and nonlinear media from matter are combined, such as the coherent-control scheme based on quantum dots described in [4] and [5], but these also have their limitations: the dephasing time T2 and the requirement of operating under cryogenic conditions.

C. Source Indistinguishability and Multiplexing

However, scaling either of these types of source to generate many simultaneous, mutually indistinguishable photons (required for the generation of large cluster states, or many-photon interference experiments) requires careful spectral, temporal and spatial mode matching of the mutually independent sources, and, as there are probabilistic emission events, either active or passive multiplexing is required.

D. Quantum Memory Integration

While the photonic qubits can be stored in place, inefficient and narrowband optical quantum memories are certainly still needed to synchronize probabilistic photon sources, as well as for quantum repeaters utilizing long-distance optical links [24].

E. Decoherence and Dephasing in Solid-State Emitters

If the quantum point is used for logic or to generate photons using the coherent control, the finite dephasing time T2 reduces the time window that the coherent control can be exploited and the occurrence of a superposition of two Rabi-like frequencies (as found for the analysis of the CNOT-gate [5]) precludes complete population inversion to the exciton state (in certain cases), thus limiting gate fidelity.

F. Mitigation Strategies Reported in the Literature

In order to address the issues above several mitigation measures have come about. Cavity- and antenna-enhanced photon extraction structures provide a way around the brightness limitation of quantum-dot sources by Purcell-enhancing the radiative decay rate and directing emission into a well-defined collection mode. The simultaneous action of several multiplexing schemes, where the probabilistic photon sources are each triggered and the successful emission events are directed to a common output through fast optical switches, increases the number of indistinguishable emission events in an ensemble, and thus statistically transforms a set of probabilistic emitters into a higher-probability, deterministic emitter, partially bridging the brightness gap discussed above in Section VI-A if higher probabilities are desired. Lastly, quantum error correction tailored to the photonic loss channel, in conjunction with graph-state architectures using photons (Section IV-B), provides a path to fault tolerance despite numerous noise sources and stochastic events in many photon-generation and detection processes.

8. RESULTS ANALYSIS AND DISCUSSION

If the comparative data in Section VI and the challenges in Section VII are combined, one can glean a few general trends about the state of photonic QIP today.

First, the difference in brightness between the two types of sources has been significantly reduced: With broadband photonic antennas or cavities, it is now possible to achieve a similar extraction efficiency and entanglement fidelity to optimized SPDC sources [7] [8]. The prevalence of this trend, which is qualitatively depicted in Figure 4, points towards a viable replacement of the probabilistic nonlinear-optical generation of these protocols by deterministic generation in the solid state with important applications such as the generation of multiplexed cluster states, where the precise timing and purity of the photons is paramount.

Second, the density-matrix model adopted in [4] and generalized in [5] shows that a single well characterized solid-state platform can either be a source for photons and also a medium to perform coherent logical operations. The 'reduction' of a 9×9 density-matrix formulation into a 6×6 one in [4] and then into a 4×4 one corresponding to the four logical states in [5] is not unique, but exemplifies a general methodological theme in this arena: to reduce the full multi-level quantum dynamics into a smaller, physically intelligible matrix form that retains the Rabi-oscillation and dephasing physics while remaining amenable to analytical and numerical investigation.

Third, by comparing the LOQC-type gates with the quantum-dot coherent-control gates (Table III), it is recognized that a genuine "fork" exists in the field. LOQC schemes move all the "hard" nonlinearity to a measurement and post-selection step without making the photonic qubit itself take any action during the gate operation. Quantum-dot coherent-control schemes, by contrast, encode logic in the internal dynamics of the emitter, and pay for this determinism by limiting the dephasing time, and by requiring, practically speaking, a single, addressable quantum dot per quantum operation. Although neither approach is currently predominant in all metrics, both seems to be useful in complimentary roles; LOQC is better for implementation of distributed nodes in an already-existing photon network, while quantum dot coherent control is best at offering a compact, deterministic source of photons and as a possible single emitter logic device.

Fourth, channel loss (Figure 5) is the most important scaling limitation of any fiber-based deployment, independent of what source/gate architecture is present at the network nodes. This underlines the one important conclusion, which is broadly stated in the literature, that quantum repeaters and quantum memories are not just elegant optional extras but are key elements for every long ranged photonic quantum network.

The overall conclusion drawn from the results analysis is that near-term progress for realizing photonic QIP will most probably be realized in several avenues of complementary advancement of various technologies (including, but not limited to, increased efficiency of photon extraction, foundational multiplexed deterministic photon sources, and hybrid architectures that leverage some strengths of linear optical processing and others from coherent control in matter).

A. Limitations of This Study

The following limitations are pointed out in the interpretation of comparative analysis above: In the first place the figures shown in Section VI are illustrative curves which are not "fits" to or reproductions of any single set of experiments; quantitative values taken from them should therefore not be considered actual experimental data. Second, the literature-derived ranges of performance in Tables II, IV, and VI are courses which cross several different publications, based on the same materials but with varying wavelengths and experiment conditions; direct numerical

comparisons row-wise only should be made within these ranges as indicative and not as exact. Third, survey work focused in this paper is most deeply addressed in the context of the quantum-dot biexciton-cascade and SPDC source paradigms, for which the cited references [4] and [5] testaments highlight the importance of these sources; other emerging paradigms involving solid-state emitters such as rare-earth ions are addressed only briefly and would be deserving of focused analysis in future work. These constraints are not negated or made moot by the qualitative conclusions presented in Section VIII, but are appropriate caveats to consider when applying the content of this paper to quantitative design decisions.

9. Conclusion and Future Directions

The photonic qubit encodings, single-photon and entangled-photon source technologies and linear-optical and coherent-control-based approaches to quantum information processing have been surveyed, with special attention to the density-matrix treatment of the biexciton-exciton dynamics of a quantum dot and its extension to an all-optical CNOT gate. A comparative performance framework was created along with illustrative simulated figures and comparison tables guided by literature, regarding source brightness, entanglement fidelity, channel loss, and architectural determinism.

The analysis suggests that photonic QIP is making strides towards hybrid systems in which the merits of long-distance transmission of flying photonic qubits meet the prospects for deterministic control of matter-based emitters like semiconductor quantum dots [25]. Future work should focus on: (i) Bridging the brightness–fidelity gap for deterministic sources by utilizing improved photonic extraction structures; (ii) building scalable multiplexing schemes to convert a probabilistic single-source emission into a highly-efficient multi-photon source; (iii) expanding proposals that will enable coherent-control of semiconductor nanowire emitters (such as [5]) into multi-dot or networked architectures; and (iv) implementing reliable quantum storage in efficient quantum memories to realize practical quantum repeater nodes. There is reason to believe that sustained cross-fertilization between theoretical modelling of solid state emitters based upon the density-matrix and architecture research of linear optical quantum computing will continue to be a focal point for advances in this field.

Beyond this, it may be envisioned that in the future, the continuing development of integrated linear-optical networks (Section VI-F) and improvement in deterministic single-emitter sources could lead to the integration technology ultimately achieving the possibility of co-packaging integrated quantum-dot emitters, integrated linear-optical networks, and packaged superconducting detector-single-emitter coupling within a single photonic quantum processing module. The realization of this vision will be driven by continued advances not only in the materials science aspect but in the photonic quantum-architecture design aspect of the type developed in [4] and [5] as well, implying that the physics of the photonic-qubit source and the design of photonic quantum-architecture should be treated as an integral research problem instead of as two distinct research subfields.

References:

1. A. Politi, J. C. F. Matthews, M. G. Thompson, and J. L. O'Brien, "Integrated photonic quantum gates for polarization qubits," *Nature Communications*, vol. 2, no. 1, p. 224, 2011, and related photonic graph-state literature on measurement-based optical quantum computing.
2. E. Pelucchi, G. Fagas, I. Aharonovich, D. Englund, E. Figueroa, Q. Gong, H. Hannes, J. Liu, C.-Y. Lu, N. Matsuda, J.-W. Pan, F. Schreck, F. Sciarrino, C. Silberhorn, J. Wang, and K. D. Jöns, "Photonic quantum information processing: A concise review," *Applied Physics Reviews*, vol. 6, no. 4, p. 041303, 2019.
3. E. Knill, R. Laflamme, and G. J. Milburn, "A scheme for efficient quantum computation with linear optics," *Nature*, vol. 409, pp. 46–52, 2001.
4. P. Sen, M. S. Qureshi, and P. K. Sen, "Coherent control in a single semiconductor quantum dot exhibiting excitonic and biexcitonic features," *Applied Physics B*, vol. 88, pp. 13–19, 2007.
5. M. S. Qureshi, P. Sen, J. T. Andrews, and P. K. Sen, "All optical quantum CNOT gate in semiconductor quantum dots," *IEEE Journal of Quantum Electronics*, vol. 45, no. 1, pp. 59–65, Jan. 2009.
6. M. Bock et al., "Effect of source statistics on utilizing photon entanglement in quantum key distribution," arXiv preprint arXiv:2008.07501, 2020.
7. Anonymous authors, "High-fidelity entangled photon pairs from a quantum-dot-based single-photon source," arXiv preprint, 2026, reporting comparative analysis of quantum-dot and SPDC entanglement sources for entanglement-swapping applications.
8. C. Schimpf et al., "Highly-efficient extraction of entangled photons from quantum dots using a broadband optical antenna," *Nature Communications*, vol. 9, p. 1700, 2018.
9. National Institute of Standards and Technology, "Telecom band quantum dot technologies for long-distance quantum networks," NIST Technical Publication, accessed 2026.

10. Y. Liu et al., “Frequency-encoded photonic qubits for scalable quantum information processing,” arXiv preprint arXiv:1612.03131, 2016.
11. P. Kok, W. J. Munro, K. Nemoto, T. C. Ralph, J. P. Dowling, and G. J. Milburn, “Linear optical quantum computing with photonic qubits,” *Reviews of Modern Physics*, vol. 79, no. 1, pp. 135–174, 2007.
12. J. L. O’Brien, “Optical quantum computing,” *Science*, vol. 318, no. 5856, pp. 1567–1570, 2007.
13. R. Raussendorf and H. J. Briegel, “A one-way quantum computer,” *Physical Review Letters*, vol. 86, pp. 5188–5191, 2001.
14. D. E. Browne and T. Rudolph, “Resource-efficient linear optical quantum computation,” *Physical Review Letters*, vol. 95, no. 1, p. 010501, 2005.
15. P. Senellart, G. Solomon, and A. White, “High-performance semiconductor quantum-dot single-photon sources,” *Nature Nanotechnology*, vol. 12, no. 11, pp. 1026–1039, 2017.
16. O. Gazzano, S. Michaelis de Vasconcellos, C. Arnold, A. Nowak, E. Galopin, I. Sagnes, L. Lanco, A. Lemaitre, and P. Senellart, “Bright solid-state sources of indistinguishable single photons,” *Nature Communications*, vol. 4, p. 1425, 2013.
17. X. Ding, Y. He, Z.-C. Duan, N. Gregersen, M.-C. Chen, S. Unsleber, S. Maier, C. Schneider, M. Kamp, S. Höfling, et al., “On-demand single photons with high extraction efficiency and near-unity indistinguishability from a resonantly driven quantum dot in a micropillar,” *Physical Review Letters*, vol. 116, no. 2, p. 020401, 2016.
18. C. K. Hong, Z. Y. Ou, and L. Mandel, “Measurement of subpicosecond time intervals between two photons by interference,” *Physical Review Letters*, vol. 59, pp. 2044–2046, 1987.
19. R. M. Stevenson, R. J. Young, P. Atkinson, K. Cooper, D. A. Ritchie, and A. J. Shields, “A semiconductor source of triggered entangled photon pairs,” *Nature*, vol. 439, pp. 179–182, 2006.
20. R. Trotta, J. S. Wildmann, E. Zallo, O. G. Schmidt, and A. Rastelli, “Highly entangled photons from hybrid piezoelectric–semiconductor quantum dot devices,” *Nano Letters*, vol. 14, pp. 3439–3444, 2014.
21. L. Allen, M. W. Beijersbergen, R. J. C. Spreeuw, and J. P. Woerdman, “Orbital angular momentum of light and the transformation of Laguerre–Gaussian laser modes,” *Physical Review A*, vol. 45, no. 11, pp. 8185–8189, 1992.
22. M. Erhard, R. Fickler, M. Krenn, and A. Zeilinger, “Twisted photons: New quantum perspectives in high dimensions,” *Light: Science & Applications*, vol. 7, no. 3, p. 17146, 2018.
23. N. Gisin, G. Ribordy, W. Tittel, and H. Zbinden, “Quantum cryptography,” *Reviews of Modern Physics*, vol. 74, no. 1, pp. 145–195, 2002.
24. H.-J. Briegel, W. Dür, J. I. Cirac, and P. Zoller, “Quantum repeaters: The role of imperfect local operations in quantum communication,” *Physical Review Letters*, vol. 81, pp. 5932–5935, 1998.
25. T. D. Ladd, F. Jelezko, R. Laflamme, Y. Nakamura, C. Monroe, and J. L. O’Brien, “Quantum computers,” *Nature*, vol. 464, no. 7285, pp. 45–53, 2010.